J|A|C|S
ARTICLES
Published on Web 10/29/2005

Molecular Recognition in Structured Matrixes: Control of Guest Localization in Block Copolymer Films

Roy Shenhar,[†,§] Hao Xu,[†] Benjamin L. Frankamp,[†] Thomas E. Mates,[‡] Amitav Sanyal,[†,¶] Oktay Uzun,[†] and Vincent M. Rotello*[,†]

Contribution from the Department of Chemistry, University of Massachusetts−Amherst, Amherst, Massachusetts 01003, and Department of Materials Engineering, University of California, Santa Barbara, California 93106-5050

Received August 11, 2005; E-mail: rotello@chem.umass.edu

Abstract: We demonstrate the use of molecular recognition to control the spatial distribution of guest molecules within block copolymer films. Block copolymers bearing recognition units were combined with complementary and noncomplementary molecules, and the extent of segregation of these molecules into the different domain types within microphase-separated thin films was quantitatively analyzed using dynamic secondary ion mass spectrometry (SIMS). Complementarity between the guest molecules and the polymer functionalities proved to be a key factor and an efficient tool for directing the segregation preference of the molecules to the different domain types. The effect of segregation preference on the glass transition temperature was studied using differential scanning calorimetry (DSC), and the results corroborate the SIMS findings. In a complementary study, guests with tunable sizes (via dendron substituents) were used to control block copolymer morphology. Morphological characterization using transmission electron microscopy (TEM) and X-ray diffraction reveal that selectivity differences can be directly translated into the ability to obtain different morphologies from recognition unit-functionalized block copolymer scaffolds.

Introduction

Molecular recognition provides a powerful tool for the control of self-assembly processes.[1] The combination between molecular recognition and polymers[2] has been receiving increased attention lately, as it provides facile routes to polymer functionalization,[3] incorporation of performance-enhancing additives,[4] modification of surface properties,[5] and nanoparticle assembly.[6] A different type of self-assembly mechanism is exhibited by block copolymers. Block copolymers self-organize into well-defined solid-state morphologies on the 10−100 nm scale, a property that makes them very attractive materials for nanotechnological applications.[7] Additionally, block copolymers can be used as templates for selective incorporation and ordering of inorganic nanoparticles for optical application[8,9] and for directing the segregation of additives for the creation of nano-objects,[10] mesoporous[11,12] and stimuli-responsive materials.[13]

Integration of block copolymer self-assembly with molecular recognition processes provides access to hierarchical materials with a wide range of potential applications. In recent studies, a variety of electrostatic and single-point hydrogen-bonding motifs have been used to control guest localization in block co-

[†] University of Massachusetts.
[‡] University of California.
[§] Current address: Institute of Chemistry, The Hebrew University of Jerusalem, Jerusalem, Israel 91904.
[¶] Current address: Department of Chemistry, Faculty of Arts and Sciences, Bogazici University, Bebek 80815, Istanbul, Turkey.

(1) (a) Grzybowski, B.; Whitesides, G. M. *Science* **2002**, *295*, 2418−2421. (b) Lehn, J.-M. *Supramolecular Chemistry, Concepts and Perspectives*; VCH: Weinheim, Germany, 1995. (c) Whitesides, G. M.; Mathias, J. P.; Seto, C. T. *Science* **1991**, *254*, 1312−1319. (d) Whitesides, G. M.; Simanek, E. E.; Mathias, J. P.; Seto, C. T.; Chin, D. N.; Mammen, M.; Gordon, D. M. *Acc. Chem. Res.* **1995**, *28*, 37−44 and references therein.
(2) (a) Duffy, D. J.; Das, K.; Hsu, S. L.; Penelle, J.; Rotello, V. M.; Stidham, H. D. *J. Am. Chem. Soc.* **2002**, *124*, 8290−8296. (b) Ilhan, F.; Diamondis, L.; Gautreau, L.; Rotello, V. M. *Chem. Commun.* **2000**, 447−448.
(3) (a) Pollino, J. M.; Stubbs, L. P.; Weck, M. *J. Am. Chem. Soc.* **2004**, *126*, 563−567. (b) Stubbs, L. P.; Weck, M. *Chem. Eur. J.* **2003**, *9*, 992−999. (c) Pollino, J. M.; Weck, M. *Chem. Soc. Rev.* **2005**, *34*, 193−207. (d) Ilhan, F.; Gray, M.; Rotello, V. M. *Macromolecules* **2001**, *34*, 2597−2601.
(4) Carroll, J. B.; Waddon, A. J.; Nakade, H.; Rotello, V. M. *Macromolecules* **2003**, *36*, 6289−6291.
(5) (a) Sanyal, A.; Norsten, T. B.; Uzun, O.; Rotello, V. M. *Langmuir* **2004**, *20*, 5958−5964. (b) Norsten, T. B.; Jeoung, E.; Thibault, R. J.; Rotello, V. M. *Langmuir* **2003**, *19*, 7089−7093.
(6) (a) Boal, A. K.; Ilhan, F.; DeRouchey, J. E.; Thurn-Albrecht, T.; Russell, T. P.; Rotello, V. M. *Nature* **2000**, *404*, 746−748. (b) Boal, A. K.; Gray, M.; Ilhan, F.; Clavier, G. M.; Kapitzky, L.; Rotello, V. M. *Tetrahedron* **2002**, *58*, 765−770.
(7) See, for example: (a) Park, M.; Harrison, C.; Chaikin, P. M.; Register, R. A.; Adamson, D. H. *Science* **1997**, *276*, 1401−1404. (b) Thurn-Albrecht, T.; Schotter, J.; Kästle, G. A.; Emley, N.; Shibauchi, T.; Krusin-Elbaum, L.; Guarini, K.; Black, C. T.; Tuominen, M.; Russell, T. P. *Science* **2000**, *290*, 2126−2129. (c) Chan, V. Z.-H.; Hoffman, J.; Lee, V. Y.; Iatrou, H.; Avgeropoulos, A.; Hadjichristidis, N.; Miller, R. D.; Thomas, E. L. *Science* **1999**, *286*, 1716−1719.
(8) (a) Bockstaller, M. R.; Lapetnikov, Y.; Margel, S.; Thomas, E. L. *J. Am. Chem. Soc.* **2003**, *125*, 5276−5277. (b) Bockstaller, M. R.; Thomas, E. L. *Phys. Rev. Lett.* **2004**, *93*, 166106. (c) Bockstaller, M. R.; Thomas, E. L. *J. Phys. Chem. B* **2003**, *107*, 10017−10024. (d) Fink, Y.; Urbas, A. M.; Bawendi, M. G.; Joannopoulos, J. D.; Thomas, E. L. *J. Lightwave Technol.* **1999**, *17*, 1963−1969. (e) Mattoussi, H.; Radzilowski, L. H.; Dabbousi, B. O.; Fogg, D. E.; Schrock, R. R.; Thomas, E. L.; Rubner, M. F.; Bawendi, M. G. *J. Appl. Phys.* **1999**, *86*, 4390−4399.
(9) (a) Weng, C.-C.; Wei, K.-H. *Chem. Mater.* **2003**, *15*, 2936. (b) Tsutsumi, K.; Funaki, Y.; Hirokawa, Y.; Hashimoto, T. *Langmuir* **1999**, *15*, 5200. (c) Ribbe, A. E.; Okumura, A.; Matsushige, K.; Hashimoto, T. *Macromolecules* **2001**, *34*, 8239.
(10) (a) Saito, R. *Macromolecules* **2001**, *34*, 4299−4301. (b) Ulrich, R.; Du Chesne, A.; Templin, M.; Wiesner, U. *Adv. Mater.* **1999**, *11*, 141−146.
(11) (a) Ikkala, O.; ten Brinke, G. *Chem. Commun.* **2004**, 2131−2137. (b) Ikkala, O.; ten Brinke, G. *Science* **2002**, *295*, 2407−2409. (c) Valkama, S.; Ruotsalainen, T.; Kosonen, H.; Ruokolainen, J.; Torkkeli, M.; Serimaa, R.; ten Brinke, G.; Ikkala, O. *Macromolecules* **2003**, *36*, 3986−3991.

10.1021/ja055490f CCC: $30.25

polymers.[11a,b] Extension of this research to more complex recognition elements provides a means for orthogonal assembly.[3a,c] On a fundamental level, complex recognition elements provide more effective probes for the origin of guest localization, i.e., whether segregation is due to specific interactions or whether it arises from nonspecific origins such as polarity.

This paper deals with systems consisting of recognition unit-functionalized block copolymers and guest molecules, focusing on the different segregation behavior of complementary versus highly similar noncomplementary guests. Our target in this study was to characterize the different levels of selectivity afforded by the two types of systems and to investigate the ability to use molecular recognition as a mechanism for directing guest molecules into desired domains in a single-step, spontaneous organization process. Our model system is based on a polystyrene (PS) backbone bearing 2,6-diamidopyridine (DAP) recognition units along one block as the polymer scaffold (denoted as PS-*b*-PS/DAP, Figure 1a). In its microphase-separated state, this polymer features two distinct domain types: polar PS/DAP domains and apolar homo-PS domains.[14,15] The PS/DAP domains should be highly attractive to guest molecules that are complementary to the DAP functionalities, and, to a lesser extent, to other polar molecules. The homo-PS domains, on the other hand, can incorporate molecules that are more apolar in nature.

The PS-*b*-PS/DAP polymer was combined with two series of guest molecules, each consisting of two parts: a binding functionality and a bulky substituent of variable size (Figure 1c). The binding functionality in the first series of molecules was thymine (Thy), which is complementary to the DAP units on the polymer through the cooperative formation of three hydrogen bonds (Figure 1a). The second series employed the highly analogous *N*(3)-methylthymine (MeThy), which is incapable of forming a three-point hydrogen bonding with DAP yet is quite similar in polarity to the thymine recognition unit (Figure 1b). The bulky substituent in both series was provided by benzyl ether dendrons, which nearly double in volume with each increase in generation number (denoted as G_x), and can be considered inert from a functionality standpoint (i.e., they do not compete with the Thy or MeThy moieties on the interaction with the DAP functionalities). This design allows us to determine the ability of the recognition element to dictate spatial localization to systems of varying dimensions.

In this study, we have quantified the level of selectivity and its dependence on the degree of complementarity between the guest molecules and the polymer functionalities (Figure 2). We have also demonstrated the utility of this approach for selective modification of specific domain properties using guests with dendritic substituents of varying sizes for obtaining different equilibrium morphologies from a single block copolymer scaffold (Figure 2a).

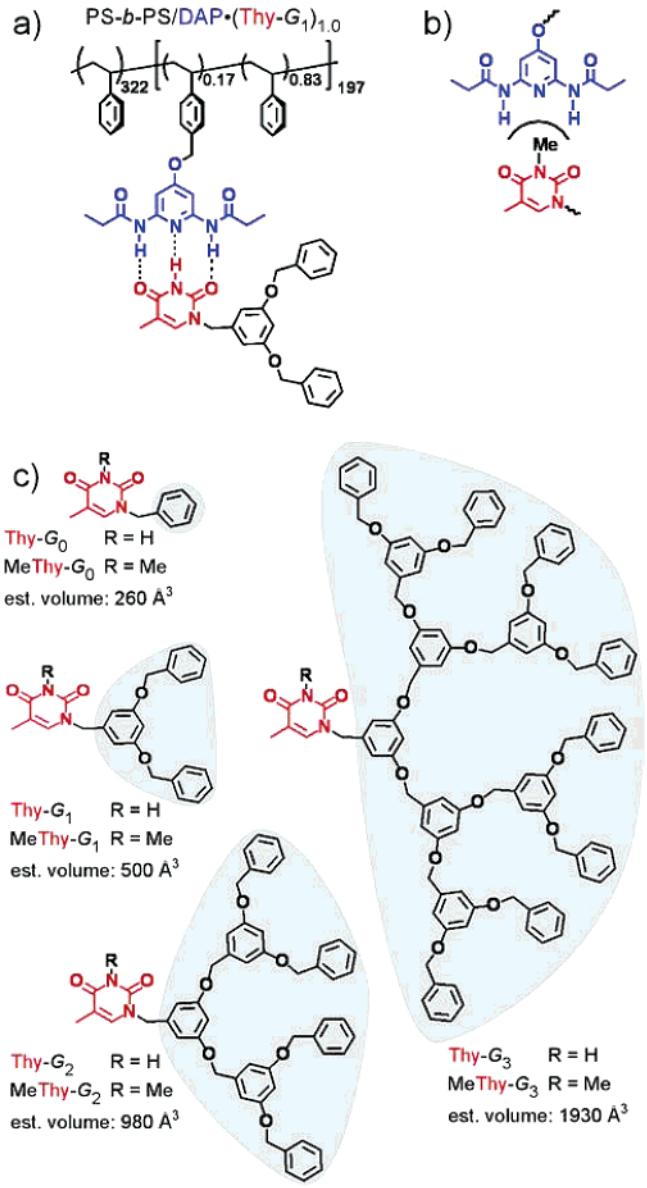

Figure 1. (a) Noncovalent functionalization of a DAP-functionalized block copolymer with a G_1-dendronized thymine molecule. (b) Noncomplementarity between a MeThy molecule and the DAP functionality. (c) Chemical structures and estimated volumes (ref 16) of the dendronized Thy and MeThy molecules, illustrating the near-exponential increase in molecular volume with generation number.

Results and Discussion

By definition, a high selectivity of a guest molecule toward a certain phase of the material means that the vast majority of the guest compounds populates the domains of that type, while only a negligible amount of these molecules segregates to domains of the other type. If the domains are arranged in periodic layers parallel to a flat substrate (as is normally the case with thin films of block copolymers cast on strongly interacting substrates[17]), then the concentration profile of the

(12) (a) Du, P.; Li, M. Q.; Douki, K.; Li, X. F.; Garcia, C. R. W.; Jain, A.; Smilgies, D. M.; Fetters, L. J.; Gruner, S. M.; Wiesner, U.; Ober, C. K. *Adv. Mater.* **2004**, *16*, 953−957. (b) Simon, P. F. W.; Ulrich, R.; Spiess, H. W.; Wiesner, U. *Chem. Mater.* **2001**, *13*, 3464−3486. (c) Templin, M.; Franck, A.; Du Chesne, A.; Leist, H.; Zhang, Y.; Ulrich, R.; Schädler, V.; Wiesner, U. *Science* **1997**, *278*, 1795−1798. (d) Garcia, C. B. W.; Zhang, Y.; Mahajan, S.; DiSalvo, F.; Wiesner, U. *J. Am. Chem. Soc.* **2003**, *125*, 13310−13311. (e) Kamperman, M.; Garcia, C. B. W.; Du, P.; Ow, H.; Wiesner, U. *J. Am. Chem. Soc.* **2004**, *126*, 14708−14709.

(13) Ruokolainen, J.; Mäkinen, R.; Torkkeli, M.; Mäkelä, T.; Serimaa, R.; ten Brinke, G.; Ikkala, O. *Science* **1998**, *280*, 557−560.

(14) Shenhar, R.; Sanyal, A.; Uzun, O.; Nakade, H.; Rotello, V. M. *Macromolecules* **2004**, *37*, 4931−4939.

(15) For simplicity, the terms "homo-PS domains" and "PS/DAP domains" will be used throughout the text to refer to the material phases consisted of the respective blocks even when these domains incorporate the guest molecules.

(16) Calculated volumes (*Spartan '02*, Wavefunction, Inc.: Irvine, CA 92612) represent average values obtained for minimized structures (molecular mechanics) of the dendronized Thy and MeThy molecules.

(17) Fasolka, M. J.; Mayes, A. M. *Annu. Rev. Mater. Res.* **2001**, *31*, 323−355.

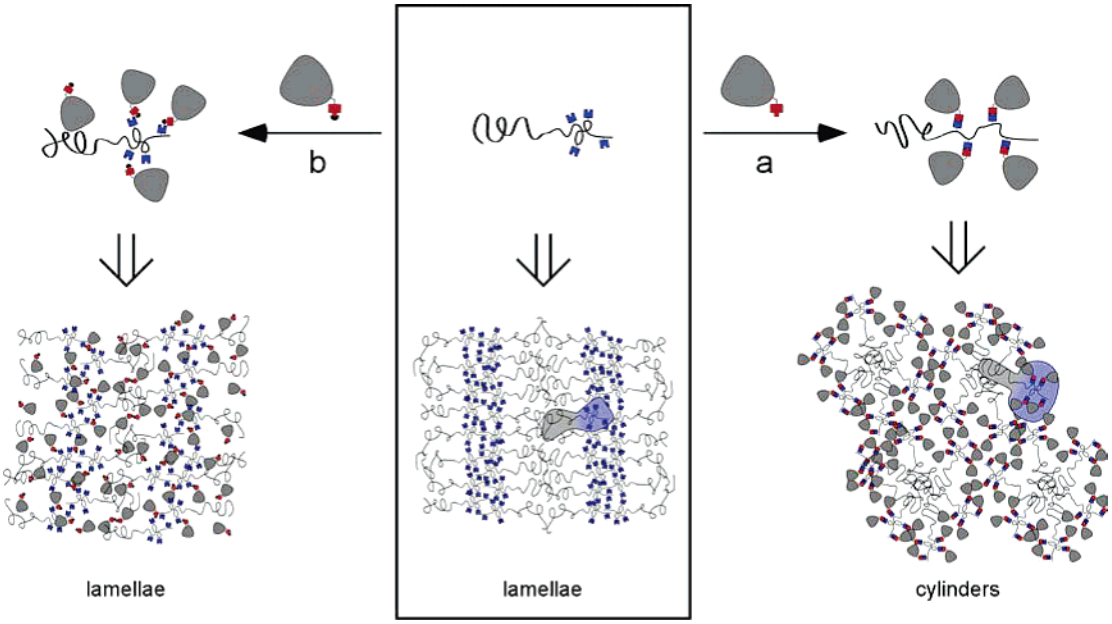

Figure 2. (a) Recognition-mediated swelling of functionalized block copolymer domains with dendritic molecules. (b) Nonspecific interactions lead to lower selectivity and retention of original morphology.

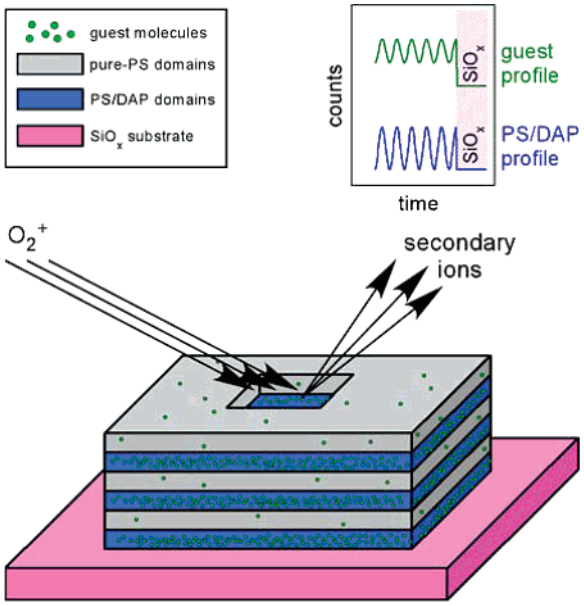

Figure 3. Schematic representation of a dynamic SIMS experiment in thin films of PS-*b*-PS/DAP•guest in the general case where the guest molecule exhibits partial selectivity toward the PS/DAP domains.

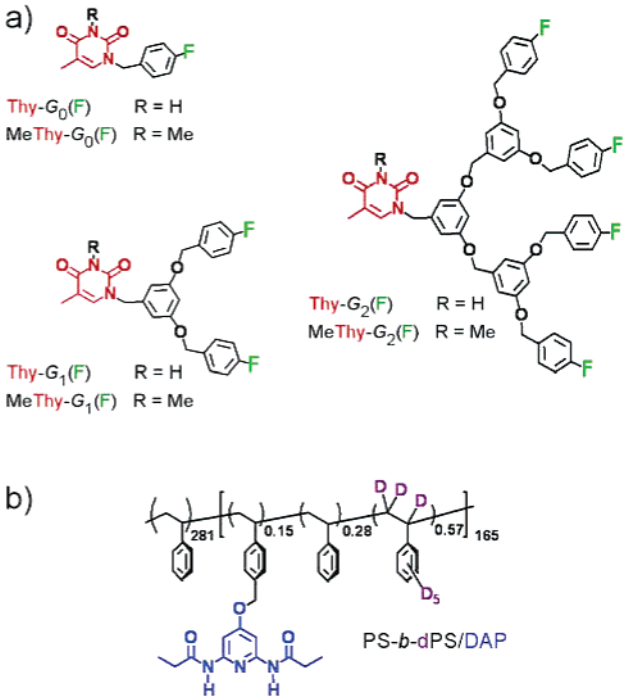

Figure 4. Chemical structures of (a) fluorine-tagged dendronized Thy and MeThy molecules and (b) partially deuterated recognition block copolymer.

components of each domain along the substrate's normal should exhibit oscillations that could be detected by a depth-profiling technique. In the system under consideration, comparing the concentration profiles of the PS/DAP block to that of the guest molecule can be used as a direct probe for selectivity (Figure 3).

Dynamic secondary ion mass spectrometry (SIMS) is a depth-profiling technique that is highly suitable for the analysis of thin polymer films.[18] During a dynamic SIMS experiment, a beam of reactive ions is used to continuously degrade a selected area in the film, and secondary ions emitted from the center of the this area are continuously detected and analyzed for mass and concentration as the etching process progresses. Proper labeling of the respective components enables the direct identification of the different domain types and guest molecules in the film with respect to depth, facilitating a quantitative determination of the molecule's concentration in each domain type. To that end, we synthesized fluorine-tagged, dendronized Thy and MeThy molecules up to generation 2 (respectively denoted as Thy-G_x(F) and MeThy-G_x(F), where x stands for the generation number and (F) denotes the fluorination, Figure 4a) and a DAP-functionalized polymer, where the functionalized

(18) Schwarz, S. A.; Wilkens, B. J.; Pudensi, M. A. A.; Rafailovich, M. H.; Sokolov, J.; Zhao, X.; Zhao, W.; Zheng, X.; Russell, T. P.; Jones, R. A. L. *Mol. Phys.* **1992**, *76*, 937−950.

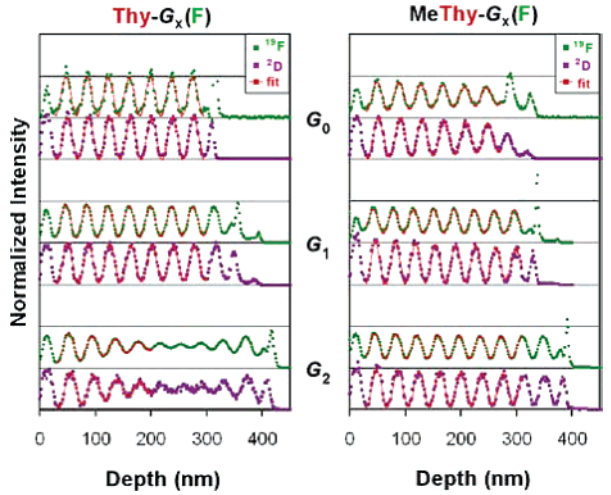

Figure 5. SIMS traces of the ^{19}F (green) and ^{2}D (purple) signals of thin films of the PS-*b*-dPS/DAP polymer with the Thy-G_x(F) and MeThy-G_x-(F) molecules (at 0.9 DAP-equivalents). All traces were normalized to obtain the same offset of their sinusoidal wave and shifted vertically for clarity.

block was partially deuterated (denoted as PS-*b*-dPS/DAP, Figure 4b).

The deuterium-labeled PS-*b*-dPS/DAP polymer (M_n 52 300 Da, 24 DAP units per chain on average, estimated volume fraction of DAP-functionalized block, $f_{dPS/DAP} = 0.43$) was mixed with each fluorinated guest at 0.9 DAP-equivalents in chloroform solutions, spin-cast on SiO_x chips, and annealed at 130 °C for 4 h. The polymer was specifically designed, in terms of both the volume fraction of the dPS/DAP block and the relatively low number of functionalities, to exhibit a lamellar morphology in most mixtures. Small-angle X-ray scattering (SAXS) analysis[19] revealed that the lamellar morphology was indeed obtained in all mixtures but that of Thy-G_2(F) (the largest complementary fluorinated guest, which gave rise to cylinders). In addition, mixing the guests at a slightly less than 1:1 guest/DAP ratios was done to avoid excess of guest molecules, which further complicates the system of interactions.

The normalized SIMS traces of emitted ^{19}F and ^{2}D anions for each of the six mixtures (Figure 5) exhibit sinusoidal characteristics, indicative of sinusoidal or near-sinusoidal concentration profiles.[20] The depth-wise locations of layers with high content of fluorinated guests correlate well with the locations of the dPS/DAP domains (indicated by high ^{19}F and ^{2}D intensities, respectively).[21] This correlation indicates the general preference (of different degrees, nonetheless) of both the Thy and MeThy derivatives toward the dPS/DAP domains.[22]

The SIMS traces of the Thy-G_2(F) film are qualitatively different from the rest, showing dampening of the oscillations near the center of the film. This behavior arises from the cylindrical morphology of the Thy-G_2(F) film. The oscillation dampening results from an increased abundance of topological defects in the cylindrical morphology compared to that in the lamellar morphology, which is expected from interfacial area considerations.[23,24]

To quantify the degree of selectivity in each of the mixtures, the sinusoidal characteristics of the SIMS traces were extracted by fitting the data to the following function:

$$I(h) = (-\alpha h + 1)\, A \sin(\omega h + \phi) + C \qquad (1)$$

where h is the depth of etching. The normalized linear decay multiplier was added to account for small charging effects noticed in some of the samples and was used also for the analysis of the traces of Thy-G_2(F) (assuming a linear dependence in both cases). Fitting was done over the regions in the traces that correspond to the bulk of the films, where the concentration profiles were largely unaffected by the interfaces (see Figure 5).

Among the few parameters that describe each sinusoidal wave, the most meaningful for the selectivity analysis are the amplitude (A) and the vertical offset (C). In the simplest treatment, the amplitude and offset correspond, respectively, to the difference in concentration of the element along the film's normal and to the average concentration of the analyzed element in the film. The physical meaning of A and C dictates that $A \leq C$ in concentration profiles that follow a true sinusoidal dependence. The ratio $R = A/C$ can thus be used as a concentration-normalized spatial distribution parameter of the analyzed element within the film. For example, an element existing exclusively in one domain type will exhibit SIMS oscillations that reach zero at their minima (see Figure 3, blue curve), in which case the value of A will approach the value of C, and the calculated spatial distribution parameter (R) will be close to unity. Conversely, a totally uniform distribution of the element between the two domain types, which would be manifested by a constant depth profile (i.e., $A = 0$), would result in $R = 0$ (an intermediate situation is depicted in Figure 3, green curve).

Table 1 lists the calculated spatial distribution parameters for the ^{2}D and ^{19}F elements in each film. As expected, the calculated values of R(D) in most samples are close to unity,[25] reflecting the strong segregation of the PS and dPS/DAP blocks into distinct spatial domains. In comparison, the R values calculated for the ^{19}F traces are somewhat lower than the corresponding R(D) values, indicating the smaller degree of segregation of the fluorinated molecules into distinct layers. Importantly, it is noticed that the R(F) values calculated for the MeThy-G_x(F) mixtures are substantially lower than those calculated for the Thy-G_x(F) mixtures, evidencing a closer-to-uniform distribution of the MeThy-G_x(F) molecules within the film.

(19) See the Supporting Information.
(20) Concentration profiles with more distinctive alternating "high" and "low" regions would still appear sinusoidal due to the experimental blurring caused by the limited SIMS depth resolution (ca. 6−8 nm).
(21) The reason for the apparent slight shift of the ^{19}F oscillations towards shorter etching times (which are translated to depths in Figure 5) compared to the ^{2}D oscillations is not well understood. A plausible explanation could be that the ^{19}F anions, being more stable than the ^{2}D anions, are formed and emitted slightly faster than the ^{2}D anions during the etching process.
(22) Additional common features that are observed are the low concentration of ^{2}D and ^{19}F at the top of each film and the high concentration of these elements at the polymer/SiO_x interface. These features indicate the formation of a homo-PS layer at the free surface and the formation of a dPS/DAP layer near the substrate (i.e., antisymmetric wetting conditions), which is in line with the expected lower surface tension of PS compared to that of dPS/DAP and concomitant with the stronger interaction of the polar dPS/DAP with the hydrophilic SiO_x substrate.
(23) In volume-asymmetric block copolymer systems, the formation of cylinders is preferred over the formation of asymmetric lamellae because cylinders exhibit a lower interfacial area. As a result, morphological defects would be more abundant in the cylindrical morphology than in the lamellar morphology since the overall enthalpic penalty involved will be smaller in cylinders.
(24) This phenomenon is also known in the spherical morphology, see: Yokoyama, H.; Mates, T. E.; Kramer, E. J. *Macromolecules* **2000**, *33*, 1888−1898.
(25) The value of R(D) calculated for MeThy-G_1 is 1.09, which significantly exceeds unity. This numeric artifact is attributed to the noticeable charging effect observed in this sample, which apparently deviates from linearity.

Table 1. Spatial Distribution Parameters (R) and Selectivity Parameters (S), Calculated from the SIMS Traces

	Thy-G_0(F)	Thy-G_1(F)	Thy-G_2(F)	MeThy-G_0(F)	MeThy-G_1(F)	MeThy-G_2(F)
R(F)[a]	0.93	0.82	0.89	0.75	0.56	0.62
R(D)[a]	1.02	0.95	1.01	1.01	1.09	0.97
S[b]	**0.91 ± 0.03**	**0.86 ± 0.03**	**0.88 ± 0.08**	**0.70 ± 0.04**	**0.51 ± 0.05**	**0.64 ± 0.04**

[a] Spatial distribution parameter, representing the population variation of the detected element between different spatial domains in the film (calculated as A/C, where A and C are the respective amplitude and vertical offset of the fitted sinusoidal wave). [b] Selectivity parameter, representing the degree of matching between the normalized ^{19}F and ^{2}D traces [calculated as R(F)/R(D), errors calculated from the respective curve fitting errors of the A and C parameters].

As noted previously, the peaks of the ^{19}F traces appear at similar positions as the peaks of the corresponding ^{2}D traces in all samples. While the overlap in the positions of the peaks with respect to depth served as evidence for the general selectivity of the added molecules toward the dPS/DAP domains, the *degree* of selectivity can be determined by the extent of intensity overlap of the normalized ^{19}F and ^{2}D traces in each case. The selectivity parameter, S, was therefore defined as the ratio between the spatial distribution parameters of ^{19}F and ^{2}D, i.e., $S = R(\mathrm{F})/R(\mathrm{D})$. S is also a normalized parameter: $S = 1$ indicates a perfect overlap of the normalized traces of ^{19}F and ^{2}D and, therefore, evidences a complete segregation of the fluorine-tagged molecules into the deuterium-labeled dPS/DAP domains, while a totally homogeneous distribution of the molecules within the film (i.e., with complete disregard to its microphase-separated structure) would result in $S = 0$. Since the SIMS measurement linearly relates to concentration fluctuations, the fraction of molecules that are incorporated in the homo-PS domains can be estimated as $(1 - S)/2$.

The selectivity parameters calculated for all mixtures are summarized in Table 1. All three Thy-G_x(F) mixtures exhibit high degrees of selectivity ($S \approx 0.9$, corresponding to ca. 5% nonspecific incorporation of guest molecules in the homo-PS domains), which is in line with the anticipated high efficiency of the molecular recognition interactions in these mixtures. In contrast, the MeThy-G_x(F) mixtures feature substantially lower selectivity values ($S \sim 0.5-0.7$, corresponding to 15−25% segregation of these molecules to the homo-PS domains), which are, additionally, highly dependent on the size of the dendron substituent. These differences indicate that in the MeThy-G_x-(F) systems, the MeThy−DAP interactions play a smaller role in dictating selectivity then in the Thy−DAP interaction, while the influence of the varying dendron substituents as well as entropic factors becomes more significant and facilitates a more uniform mixing.

Having characterized the effects of molecular recognition and nonspecific interactions on the distribution of guest molecules within block copolymer domains, we turned to probe the influence of the different modes of interaction on materials properties. Among the most technologically important polymer properties is the glass transition, which is the thermal transition from a hard glassy state to a soft rubbery state. The glass transition temperature (T_g) is influenced by the ability of the polymer segments to execute cooperative motions and is thus very sensitive to the local environment of the polymer chains.[26] Small molecules that are dispersed within the polymer matrix act as plasticizers, mediating the mutual interaction between neighboring chains and lowering the glass transition temperature.

Figure 6 shows differential scanning calorimetry (DSC) scans of the PS-*b*-PS/DAP block copolymer alone and with the different types of guest molecules. For comparison, we have also analyzed mixtures of a PS/DAP random copolymer (M_n 14 000 Da, 25 DAP units per chain on average), which is analogous to the PS/DAP block in the block copolymer and enables isolating the effect on the functionalized block from the effect on the entire block copolymer (Figure 6, left pane). The T_g of the PS/DAP "monoblock" is 125 °C, which is higher by 25 °C from that of PS (lit. 100 °C)[27] due to DAP−DAP dimerization.[14] Combining the PS/DAP "monoblock" with the complementary Thy-G_x guests breaks the DAP−DAP dimerization for the creation of the more favorable DAP−Thy interactions, and thus lowers the T_g. The size of the dendron substituent has an additional "lubricating" effect: while addition of Thy-G_0 only lowers the T_g to 101 °C (close to that of PS), the increasing dendron size in the larger guests apparently facilitates reducing the "friction" between neighboring chains and thus gradually lowers the T_g down to 64 °C for Thy-G_3 (Figure 6, left pane). It should be noted, however, that the glass transitions in all cases are relatively sharp, indicating normal polymer behavior. This observation suggests, therefore, that the Thy-G_x guests that accompany each polymer chain are strongly bound to it and move with it as a single entity.

In comparison to the Thy-G_x case, adding the noncomplementary MeThy-G_x results in a much stronger effect on T_g.

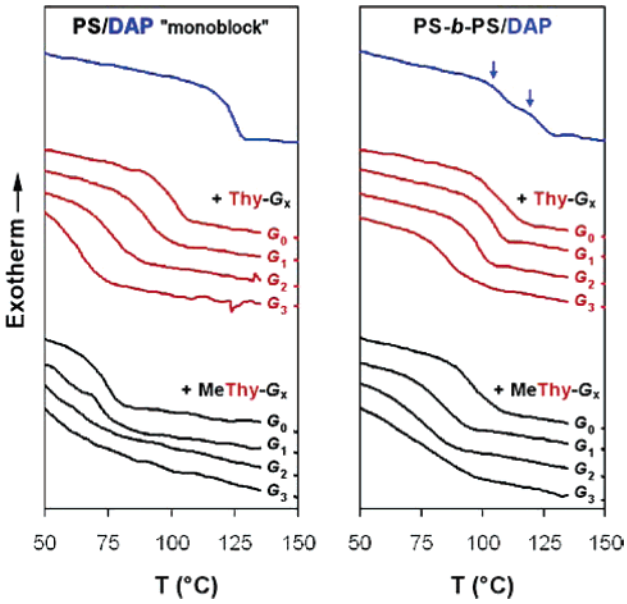

Figure 6. DSC scans of PS/DAP "monoblock" (left pane) and PS-*b*-PS/DAP (right pane) with Thy-G_x and MeThy-G_x (at 0.8 DAP-equivalents). The blue curves represent the DSC scans of the polymers without guests. The arrows indicate the locations of the glass transitions corresponding to the homo-PS and the PS/DAP phases of the PS-*b*-PS/DAP (109 and 126 °C, respectively). Curves are offset for clarity.

(26) Donth, E. *The Glass Transition: Relaxation Dynamics in Liquids and Disordered Materials*; Springer: New York, 2001.

(27) *Polymer Handbook*, 4th ed.; Brandrup, J., Immergut, E. H., Grulke, E. A., Eds.; Wiley-Interscience: New York, 1999.

Mixing the PS/DAP "monoblock" with MeThy-G_0 lowers the T_g to 74 °C, and with larger MeThy-G_x the glass transitions occur at lower temperatures. More importantly, the transitions for large MeThy-G_x appear much broader and ill-defined (Figure 6, left pane). This phenomenon indicates that the noncomplementary guests, although still mediating the DAP−DAP dimerization, are not specifically associated with the DAP functionalities as the Thy-G_x guests, and are rather dispersed within the polymer matrix, acting as "regular" plasticizers.

The block copolymer exhibits two transitions, at 109 and 126 °C, corresponding to the softening of the homo-PS and the PS/DAP phases, respectively (Figure 6, right pane).[14] Upon the addition of Thy-G_x guests only one transition remains, occurring at temperatures close to that of pure PS for Thy-G_x up to generation 2 (111, 104, and 99 °C for Thy-G_0, Thy-G_1, and Thy-G_2, respectively) and at 84 °C for Thy-G_3. This observation suggests that the homo-PS domains remain almost guest-free in most cases and thus continue to exhibit a near-constant T_g that is only slightly influenced by the plasticized PS/DAP domains. This description is in complete agreement with the SIMS results. In comparison, the T_g lowering with increasing dendron size is much steeper for mixtures containing the noncomplementary MeThy-G_x guests (95, 83, and 76 °C for MeThy-G_0, MeThy-G_1, and MeThy-G_2, respectively), ending with a very broad transition for MeThy-G_3. The strong deviation of the mixtures' glass transition temperatures from the known T_g of pure PS suggests that a large number of MeThy-G_x molecules segregate to the homo-PS domains, directly leading to its plasticization. This conclusion, as well, is supported by the SIMS results.

The quantitative selectivity analysis afforded by the SIMS demonstrates the high fidelity of polymer functionalization that can be achieved through molecular recognition (as compared to polar interactions). Furthermore, it enables treating the complementary guests as building blocks that could be "plugged" into the polymer functionalities.[3,4] Taking advantage of our original design, where guest molecules differ substantially in volume, we set out to investigate our ability to control the equilibrium morphology of a recognition block copolymer by selectively swelling[11,28] the DAP-functionalized block using the dendritic guests.

The PS-*b*-PS/DAP used (M_n 62 200 Da, 33 DAP units per chain on average, Figure 1) self-organizes upon annealing into alternating lamellae (32.6 nm period) of PS/DAP and homo-PS domains, in agreement with the estimated volume fraction of the DAP-functionalized block, $f_{PS/DAP} = 0.45$.[14] This polymer, compared to its deuterated analogue used for the SIMS study, features a larger number of DAP functionalities per chain that facilitates a faster increase in the effective volume of the PS/DAP block (and hence an earlier morphological change) when guest molecules associate with the DAP functionalities. Each of the dendritic guest molecules (Thy-G_x and MeThy-G_x) was mixed with the polymer in chloroform solutions at 1:1 guest/DAP ratio, dried, and annealed at 130 °C for ca. 16 h.

Figure 7 shows transmission electron microscopy (TEM) images of sections made from the equilibrated, solid-state mixtures. In the Thy-G_x mixtures, the morphology changed from lamellar (Thy-G_0) to cylindrical (Thy-G_1 and Thy-G_2) to spherical (Thy-G_3). The different morphologies obtained in each mixture indicate that the addition of increasingly larger dendronized thymine derivatives resulted in a progressive increase

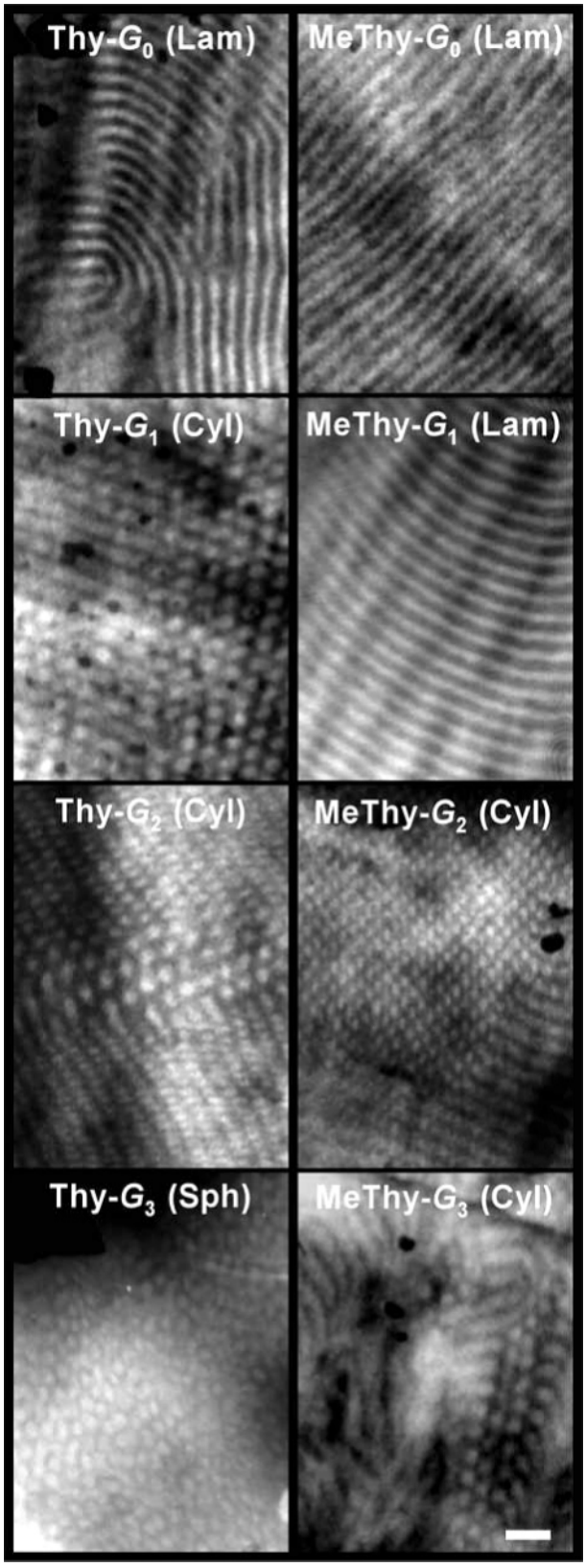

Figure 7. TEM images of 60-nm sections of block copolymer mixtures with Thy-G_x and MeThy-G_x at 1:1 guest/DAP ratios. Light features correspond to the unstained, homo-PS domains. Scale bar: 100 nm.

(28) (a) Wilney, K. I.; Thomas, E. L.; Fetters, L. J. *Macromolecules* **1992**, *25*, 2645−2650. (b) Vavasour, J. D.; Whitmore, M. D. *Macromolecules* **2001**, *34*, 3471−3483. (c) Likhtman, A. E.; Semenov, A. N. *Macromolecules* **1997**, *30*, 7273−7278.

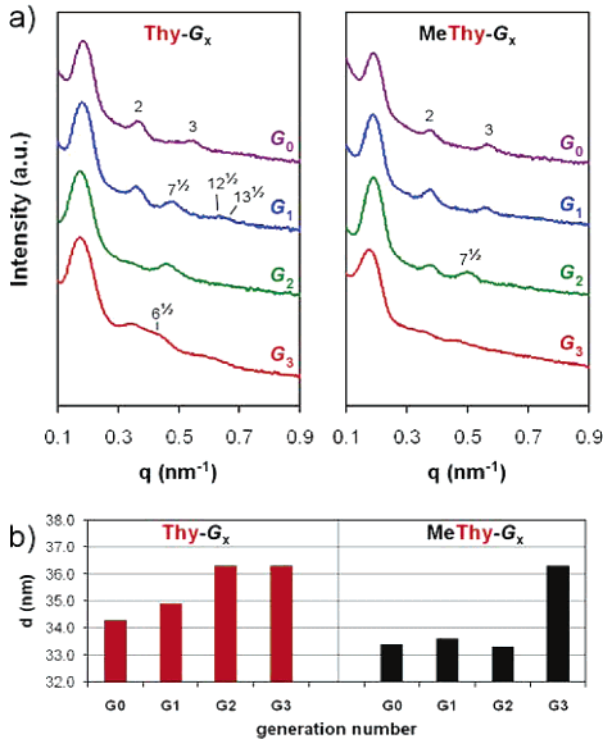

Figure 8. (a) SAXS curves of solid-state mixtures of PS-*b*-PS/DAP with Thy-G_x and MeThy-G_x; relative locations of secondary maxima with respect to the main reflection are annotated. Curves are offset for clarity. (b) Periodicities calculated from the positions of the first diffraction peaks (as $2\pi/q$).

in the effective volume fraction of the PS/DAP block, crossing the lamellar/cylindrical phase boundary at generation 1 and the cylindrical/spherical phase boundary at generation 3. In comparison, mixing with MeThy-G_x induced a slower morphology change: the lamellar morphology persisted through MeThy-G_0 and MeThy-G_1, and cylinders were observed with MeThy-G_2 and also with MeThy-G_3.

The morphology change observed in the MeThy-G_x case indicates that these molecules also segregate with some preference to the PS/DAP domain type (as also indicated by SIMS). The apparent difference between the morphology changes in both cases, however, indicates different *degrees* of selectivity of the Thy-G_x and MeThy-G_x toward the PS/DAP domains. The fact that the morphologies induced by the MeThy-G_x lag behind those of the Thy-G_x by one generation number means that to change the morphology in the same manner, the MeThy derivative has to be approximately twice as large as the corresponding Thy derivative. This behavior indicates that a larger fraction of the MeThy-G_x molecules were nonspecifically incorporated in the homo-PS domains in the corresponding mixtures compared to when Thy-G_x molecules of the same generation number were used. Therefore, a higher degree of selectivity is afforded by molecular recognition of the dendronized Thy molecules toward the PS/DAP domains, in complete agreement with the concentration variation data directly obtained from the dynamic SIMS analysis.

Small-angle X-ray scattering (SAXS) patterns (Figure 8) corroborate the morphologies inferred by the TEM images.[29] Additionally, the periodicities calculated from the SAXS curves (Figure 8b) reveal another distinction between the Thy-G_x and MeThy-G_x cases. The calculated periodicities exhibited by the MeThy-G_x mixtures are almost identical (33.4 ± 0.2 nm) up to generation 2, while those exhibited by the Thy-G_x mixtures are substantially higher (in the range of 34.0−36.6 nm) and scale-up monotonically with generation number. Taking into account that in dendronized polymers the increased congestion about the backbone leads to extended chain conformations,[30] this evidence serves as another indication that Thy-G_x associates in larger numbers with the PS/DAP blocks than MeThy-G_x.

Conclusions

Using dynamic SIMS, DSC, TEM, and SAXS analyses, we have demonstrated the considerable selectivity difference between complementary and noncomplementary systems in structured polymeric matrixes. We have also demonstrated that this difference in selectivity between complementary and noncomplementary systems can be translated into the ability (or inability) to access various morphologies from a single recognition block copolymer. This study emphasizes the crucial role of specific interactions in achieving *controlled*, noncovalent polymer functionalization. Combined with the ability to employ orthogonal functionalization schemes,[3] this methodology allows the creation of an entire set of structured functional materials from a single block copolymer.

Acknowledgment. The authors thank Professor Thomas P. Russell, Professor S. Thayumanavan, Kulandaivelu Sivanandan, and Professor Edward J. Kramer for helpful discussions, and Divya Goel for assistance with sample preparation. Financial support from the NSF [CHE-CHE-0518487 (V.R.)] and MRSEC (DMR 0213695) is gratefully acknowledged. R.S. thanks The Fulbright Foundation for a postdoctoral fellowship. B.L.F. acknowledges the ACS Division of Organic Chemistry Graduate Fellowship sponsored by The Procter and Gamble Company.

Supporting Information Available: Synthetic procedures and characterization data, additional TEM images, and SAXS data of the labeled systems (PDF). This material is available free of charge via the Internet at http://pubs.acs.org.

JA055490F

(29) Morphology is indicated in the one-dimensional diffraction curves by the relative locations of the secondary maxima on the q ordinate with respect to the first Bragg reflection. Lamellae: 1:2:3:4. Cylinders (hexagonal packing): $1:\sqrt{3}:\sqrt{4}:\sqrt{7}:\sqrt{9}:\sqrt{12}:\sqrt{13}$. Spheres (cubic packing): $1:\sqrt{2}:\sqrt{3}:\sqrt{4}:\sqrt{5}:\sqrt{6}$. Absence of peaks in the SAXS patterns is attributed to the vicinity of an overlapping form factor minimum.

(30) (a) Schlüter, A.-D.; Rabe, J. P. *Angew. Chem., Int. Ed.* **2000**, *39*, 864−883. (b) Stocker, W.; Schürmann, B. L.; Rabe, J. P.; Förster, S.; Lindner, P.; Neubert, I.; Schlüter, A.-D. *Adv. Mater.* **1998**, *10*, 793−799. (c) Percec, V.; Ahn, C.-H.; Ungar, G.; Yeardley, D. J. P.; Möller, M.; Sheiko, S. S. *Nature* **1998**, *391*, 161−164.